



# Düzce University Journal of Science & Technology

Research Article

## A Theoretical Study on the Mechanical Significance of Mineralized Collagen Fibril Orientation in Osteonal Lamellar Bone

 Feride Şermin UTKU<sup>a,\*</sup>

<sup>a</sup> Department of Biomedical Engineering, Faculty of Engineering, Yeditepe University, İstanbul, TURKEY

\* Corresponding author's e-mail address: sermin.utku@yeditepe.edu.tr

DOI: 10.29130/dubited.761512

### ABSTRACT

In this study, the effect of orientation of mineralized collagen fibrils on bone mechanical properties relating to bone anisotropy was studied using data obtained from rehydrated lamellar bone samples. The dehydration-rehydration based and experimentally determined contraction, observed in orientations parallel and perpendicular to the osteonal axis was used to calculate bone anisotropy. The sublamellar bone model, with the layered mineralized collagen fibrils rotating at 5° was used. Following this model, the mineralized collagen layers were transformed at 5° relative to the orthogonal axes using a transform matrix. With dehydration, fibril diameter was reduced towards the mineral, forming contraction vectors. The  $x$ ,  $y$  and  $z$  intercepts for these vectors were then calculated to give the  $u$ ,  $v$  and  $w$  displacements, which gave anisotropy ratios ranging from 0.15266 to 6.55054. Compared with the experimental nanoindentation findings in the literature, there may be an indication of a correlation with the results of sublamellar arrangement at 20° angles. As the lateral indentation used in the anisotropy experiments may involve varying amounts of  $u$  and  $v$  displacements, the aspect angle of lateral indentation was evaluated in relation to the structural features of the model. This evaluation indicated the larger contribution of  $v$  displacement and thus relatively much smaller contribution of  $u$  displacement to lateral contraction. These findings indicate the significant effect of the mineralized collagen fibril arrangement on bone anisotropy.

**Keywords:** Transformation Matrix, Contraction vector, Anisotropy, Mineralized Collagen Fibril Orientation.

## Osteonal Lamellar Kemikte Mineralize Kolajen Fibril Yönlenmesinin Mekanik Önemi Üzerine Teorik Çalışma

### ÖZET

Bu çalışmada, dehidrasyon-rehidrasyon sonrasında lameler kemik örneklerinden elde edilen veriler kullanılarak, mineralize kolajen fibril yönlenmesinin kemiğin mekanik özelliklerine olan etkisi incelenmiştir. Dehidrasyon-rehidrasyon sonrasında kemiğin osteonal eksenine paralel olan ve dik kesen yönlerde deneysel olarak gelişen çekme kullanılarak, kemiğin anizotropik özellikleri hesaplanmıştır. Sublameller kemik modelinde mineralize kolajen fibrilleri katmanlar halinde ve 5 derecelik açılarla rotasyon yapacak şekilde modellenmiştir. Bu modele göre, mineralize kolajen tabakaları, transformasyon matrisi kullanılarak ortogonal eksenlere 5° açı yapacak şekilde dönüştürülmüştür. Dehidrasyon sonucunda fibril çapı mineral doğrultusunda daralmış, çekmeye bağlı bir deplasman vektörü oluşturmuştur. Vektörlerin  $x$ ,  $y$  ve  $z$  eksenlerindeki izdüşümleri,  $u$ ,  $v$  ve  $w$  deplasmanları hesaplanarak, 0,15266-6,55054 aralığında anizotropi oranları bulunmuştur. Literatürdeki deneysel nanoindentasyon verileriyle kıyaslandığında, sonuçlar, sublamellerin yaklaşık 20 derecelik açılarla düzenlenmiş olabileceğini göstermiştir. Anizotropi deneylerinin bir unsuru olan lateral indentasyon farklı oranlarda  $u$  ve  $v$  deplasmanları içerebileceğinden, lateral indentasyon açısı modelin yapısal özellikleri bağlamında

değerlendirilmiştir. Bu değerlendirmenin sonucunda, v deplasmanının lateral çekmeye u deplasmanından daha fazla katkıda bulunduğu görülmektedir. Bulgular, mineralize kolajen fibrillerinin sublamellar düzenlenmesinin kemiğin anizotropisine olan önemli katkısını göstermektedir.

*Anahtar Kelimeler: Transformasyon Matrisi, Büzülme vektörü, Anizotropi, Mineralize Kolajen Fibril Yönlenmesi.*

## I. INTRODUCTION

As a hierarchical, anisotropic, fiber-reinforced composite, composed of organic and inorganic components within a hydrating medium [1]-[9], bone structure and the lamellar organization of collagen fibrils have been studied using various indentation techniques at different levels of scale [10].

At the most basic level, the bone mineral and the collagen fibril associate with each other and form the higher organized, hierarchical structures ranging from the sublamellae to lamellae, osteons and other higher lamellar structures. The bone lamella (6-8  $\mu\text{m}$  thick) (Fig. 1) consists of 2-3  $\mu\text{m}$  thick sublamellae [9] organized in a fanning arrangement [9],[11]. The collagen fibrils rotate in relation to the lamellar front in 2D, and the mineral planes [9],[11] rotate in relation to both the collagen fibrils and the lamellar front in 3D [12]-[15]. The 23 wt% collagen fibrils and the 65 wt% mineral are hydrated by 12 wt% bone fluid [5],[12],[16]-[20], present in the gaps within the fibril, between the fibrils and the fibers [13],[21]-[26]. The collagenous layers [8],[2],[23], the level of mineralization as well as the mineral plate orientation [27]-[28] determine bone mechanical behavior as displayed in the nanoindentation studies [29]-[31].

The dehydration caused dimensional changes in bone have been studied in the environmental scanning electron microscope (ESEM) as wet, dry and rehydrated samples [8]. The results of that study have indicated that in the longitudinal (Plane 2 in Fig. 1) and transverse (Plane 1 in Fig. 1) cross-sections of bone, if the specified length of a given segment is measured perpendicular and parallel to the lamellae before and after dehydration, the difference in length varies as a function of the orientation of that segment. In the longitudinal cross-sections exposing Plane 2 in Fig. 1, radially  $1.19\pm 0.78\%$  and axially  $-0.12\pm 0.75\%$ , and in the transverse cross-sections exposing Plane 1 in Fig. 1, radially  $1.39\pm 0.87\%$  and tangentially  $1.41\pm 0.57\%$  change in dimension has been observed at 28% relative humidity under the ESEM [8]. The axial contraction results have displayed a high standard deviation and a wide range ( $-4.64\%$  to  $4.52\%$ ).

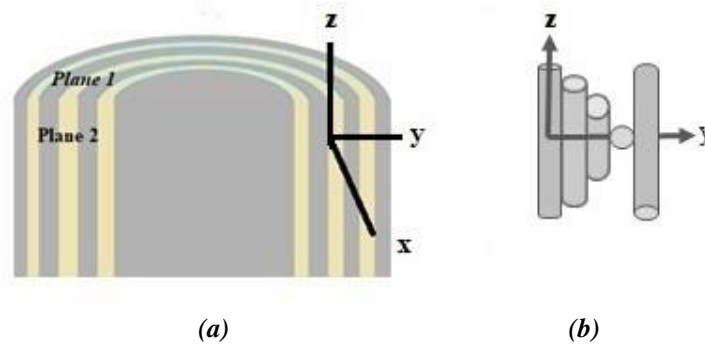


**Figure 1.** (a) Osteonal bone lamellae are displayed as striped layers, with each stripe (designating a lamella) containing the sublamellae of mineralized collagen fibrils [11]. As a result of dehydration, contraction in the organic content is displayed as axial displacement, where  $w$  is axially oriented along the long shaft of bone (along the  $z$  axis), displacement  $v$  is radially oriented (along the  $y$  axis), and displacement  $u$  is tangentially oriented (along the  $x$  axis). Plane 1 indicates the transverse surface cut of the long axis of bone and Plane 2 indicates the surface exposed by the longitudinal cut along the long bone. (b) depiction of the sublamellae within the lamella given in (a) as yellow or gray stripes.

In that study, the change in dimension was considered to be due to loss of water in the organic component (Fig. 2a). Therefore, in this study, with dehydration, the soft organic component of the mineralized collagen fibril (MCF) is assumed to contract towards the hard inorganic component (Fig. 2b); thus, creating a directional contraction, which is termed as a contraction vector.

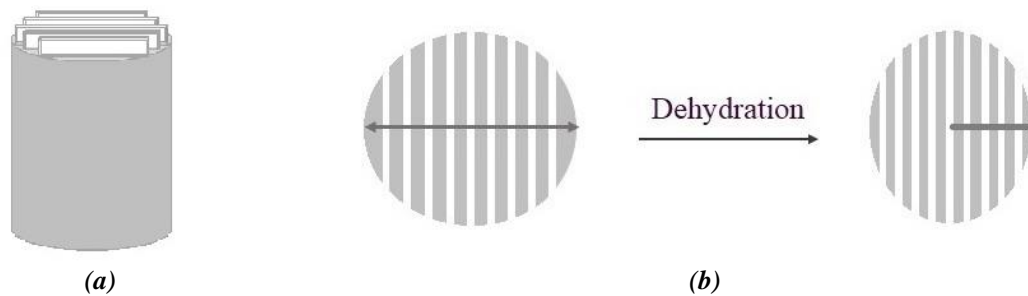


**Figure 2.** (a) The MCF depicting the mineral plates within the collagen fibril, which associates with water through hydrogen bonds. (b) The collagen fibril depicted as wet (left) and dry (right) where the plates approach each other having lost the water within and between the collagen fibrils and the plates. As the reduction in diameter is guided by the mineral plate and is directional, it is named as the contraction vector. The organic matrix in each MCF contracts (loses dimension) towards the mineral plate contained within that fibril. Here, the direction of contraction, termed as the contraction vector, is marked with an arrow.

Using the basic osteonal lamellar bone model of rotated plywood collagen fibrils [11], the indirect effect of water on bone mechanical properties was theoretically studied at the lamellar length scale. This was carried out by studying the percent change in dimension taking place between dehydrated and rehydrated osteonal lamellar bone models with collagen fibrils oriented at various angles. The results obtained here were compared with the literature [10],[29]-[31] on dimensional changes that occur in the osteonal lamellar bone with dehydration and rehydration.

## **II. MATERIALS AND METHODS**

### **A. MATERIALS**

The working model considered here, i.e. the rotated plywood model, is a single lamella of an osteonal long bone with the axially, tangentially and radially oriented MCFs (with the main orientation being axial (z-axis) and tangential (x-axis)) [2,15]. Radial (y-axis) orientation of fibrils is observed mainly along the canaliculi and Volkman's canals [4]. According to this model, the collagen fibrils are stacked radially rotating at about 30° angles and the mineral plates within each collagen fibril rotating at 30° angles about themselves [11].

### **B. METHODS**

#### **B. 1. Modification of the Model**

Here, the standard rotated plywood model of osteonal bone was modified to consist of twenty-five sublamellae (S), with collagen fibrils (S-0 to S-24) stacked about the y-axis at 5° angles on the x-z plane. The axially oriented collagen fibrils of 0° sublamella (S-0, along the z-axis [001]), rotated about the y-axis at 5° rotation steps through the 90° sublamellae (S-18, along the y-axis [100]) and up to S-24 at 120° (Fig. 3a).

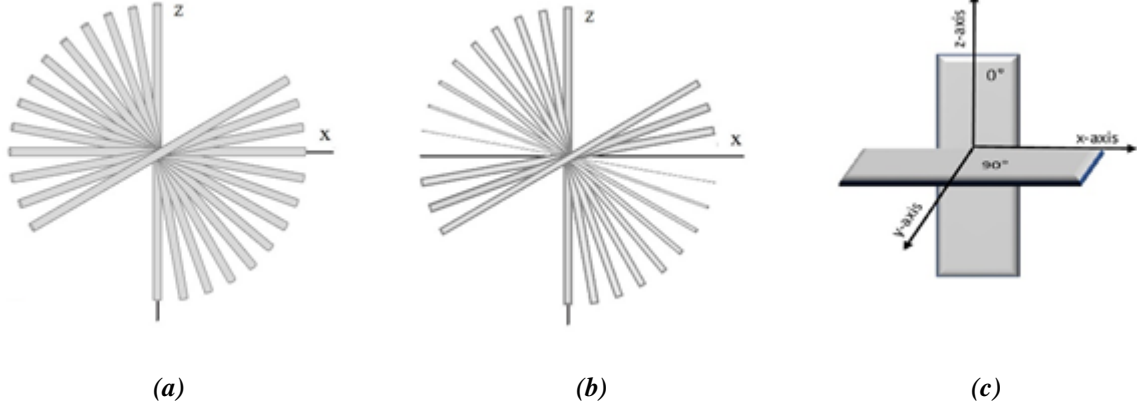


**Figure 3.** (a) the collagen fibrils of the sublamellae (of a lamella) stacked about the y axis, with fibrils rotating at 5° angles on the x-z plane, (b,c) the mineral plates of the collagen fibrils stacked along the y axis, with mineral plates rotating at 5° angles not only on the x-z plane, but also about themselves.

The mineral planes were angulated at 5° intervals ranging between 0°-120°. The mineral plate contained in the S-0 collagen fibril was oriented to intercept the y-axis at the origin forming the (010) plane (Fig. 3b-c), while the mineral plate contained in the S-18 collagen fibril was oriented to intercept the z-axis forming the mineral plane (001). The mineral planes were transformed in 3D about the x, y and z axes at 5° angles within the fibril of each sublamella, from 0° up to 90° (S-0 to S-18) and repeat the values of 5° up to 30° angles between S- 20 to S-24.

The generalized average orientations and angular rotations for the collagen fibrils and mineral planes are obtained using the transformation matrix given in equations (eqs. 1-7) within the 0°-120° range.

$$T_x = \begin{pmatrix} 1 & 0 & 0 \\ 0 & \cos \theta & -\sin \theta \\ 0 & \sin \theta & \cos \theta \end{pmatrix} \quad (1)$$

$$T_y = \begin{pmatrix} \cos \theta & 0 & \sin \theta \\ 0 & 1 & 0 \\ -\sin \theta & 0 & \cos \theta \end{pmatrix} \quad (2)$$

$$T_z = \begin{pmatrix} \cos \theta & -\sin \theta & 0 \\ \sin \theta & \cos \theta & 0 \\ 0 & 0 & 1 \end{pmatrix} \quad (3)$$

$$n_y = \begin{pmatrix} 1 \\ 0 \\ 0 \end{pmatrix} \quad (4)$$

$$n_z = \begin{pmatrix} 0 \\ 1 \\ 0 \end{pmatrix} \quad (5)$$

$$\text{Collagen fibril orientation represented by a unit vector} = T_y * n_z \quad (6)$$

$$\text{Contraction in collagen fibril represented by a unit vector} = T_y * T_x * T_z * n_y \quad (7)$$

$T_x$ ,  $T_y$ , and  $T_z$  denote the transformation matrices with respect to the x, y and z axes, while  $n_y$  and  $n_z$  denote the vectors oriented along the y and z axes. The orientation of the collagen fibril was calculated using eq. 6; while the transformation of the mineral plate orientation (indicating contraction of the collagen fibril towards the mineral plate) was calculated using eq. 7. The contraction in the oriented MCFs was then studied intermittently at every 5°, 10°, 15°, 20°, 30° or 40° angles from 0° up to 120°.

## B. 2. Calculation of Dimensional Change

The 1.4% peraxial dimensional change in sublamella [8] was calculated for the  $5^\circ$  angles, assuming that the direction of contraction is normal to the mineral plate. The peraxial projection of the contraction vector of the dehydrated fibril was given as  $u_a$ ,  $v_a$  and  $w_a$  using the transformation matrices. Contraction as displacement (given as the absolute values of  $u_a$ ,  $v_a$  and  $w_a$ ) was summed at the angles stated above to give  $u_{at}$  (sum of all  $u_a$ ),  $v_{at}$  (sum of all  $v_a$ ), and  $w_{at}$  (sum of all  $w_a$ ). Total contraction per axis was calculated in units by multiplying the radius of a collagen fibril,  $r$ , by 1.4%, and then, by the sum of displacements in the respective axes, using eq. 8. For a total displacement in the x axis,

$$u_{at} = r'(\sum u(a)) \quad (8)$$

where  $r'$  is the magnitude of contraction of the collagen fibril and  $a$  is the angle. For  $a=40^\circ$ ,  $u_{40t} = r'(\sum u(40^\circ))$  is the sum of displacements in multiples of  $40^\circ$  angles (Fig. 3). The reasoning behind this summation is that dehydration is a cumulative process, leading to the warping of bone samples.

## B. 3. Calculation of Anisotropy Ratios

The amount of contraction was then used to calculate the mechanical anisotropy in the osteonal lamellae. These results were compared with the anisotropy of elastic modulus data obtained by nanoindentation (where the elastic modulus for Plane 1 was divided by that of Plane 2 as shown in Fig. 4a) [10]. Similarly, here, the anisotropy ratios (AnR) for the sum of contraction values for Plane 1 ( $w_{at}$ ) was divided by those obtained perpendicular to the osteonal axis (described as “lateral indentations” i.e., as “ $u_{at}$ ” or “ $v_{at}$ ”).

To demonstrate the possible variation in experimental data acquired by nanoindentation due to the aspect of the indenter to the sublamellae in the study of Faingold et al. [10], here, the effect of lateral indentation direction in Plane 2 (Fig. 4a) was evaluated where the indenter aspect angle varied between angles  $0^\circ$  through  $120^\circ$  (Fig. 4b). The purpose was to determine the effect of lamellar features on the anisotropy ratios as the lateral indenter moves from the y-axis alignment to the x-axis alignment and further.

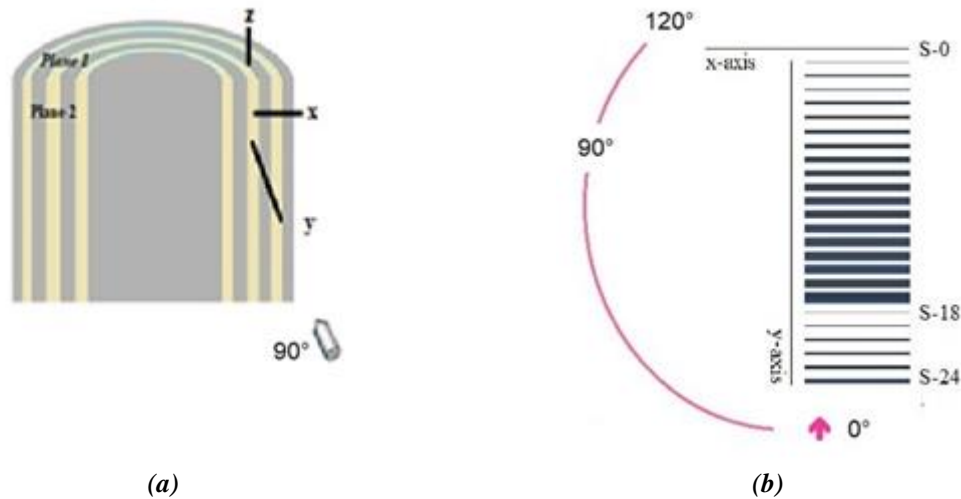


**Figure 4.** (a) The nanoindentor probe approaches Plane 2 perpendicularly, normal to the bone surface. (b) The sublamellar layers as observed in a transverse cross-section, or along the z-axis. As depicted in Figure 4a, although the nanoindentor probe approaches the surface perpendicularly, it may intercept the MCFs of the sublamellae at angles ranging from  $0^\circ$  to  $120^\circ$ . Thus, the major elastic contribution to indentation varies as a function of the intercepted MCF angle.

## III. RESULTS

The results of this study indicate that the radius of the MCF ( $r$ ), taken as 1 unit (or 1.5 nm) in the hydrated state, contracted by 1.4%, to give the contraction magnitude ( $r'$ ) of 0.014 units. Using the transformation matrices and unit vectors (eqs. 1-7), the 5° sublamellar collagen fibril angulations about the y-axis and the contraction vector orientations of the minerals were calculated (eq. 8) (Table 1).

**Table 1.** Peraxial intercepts of MCF orientations and the contraction unit vector per sublamellar layer.

Sublamellar Layer	Collagen Fibril Orientations			Contraction Vector		
	X axis	Y axis	Z axis	u	v	w
S-00	0.00000	0	1.00000	0.00000	1.00000	0.00000
S-05	-0.08716	0	0.99619	0.07926	0.99240	0.09409
S-10	-0.17365	0	0.98481	0.14131	0.96985	0.19857
S-15	-0.25882	0	0.96593	0.18530	0.93301	0.30847
S-20	-0.34202	0	0.93969	0.21147	0.88302	0.41899
S-25	-0.42262	0	0.90631	0.22115	0.82139	0.52574
S-30	-0.50000	0	0.86603	0.21651	0.75000	0.62500
S-35	-0.57358	0	0.81915	0.20035	0.67101	0.71387
S-40	-0.64279	0	0.76604	0.17589	0.58682	0.79038
S-45	-0.70711	0	0.70711	0.14645	0.50000	0.85355
S-50	-0.76604	0	0.64279	0.11520	0.41318	0.90334
S-55	-0.81915	0	0.57358	0.08497	0.32899	0.94050
S-60	-0.86603	0	0.50000	0.05801	0.25000	0.96651
S-65	-0.90631	0	0.42262	0.03589	0.17861	0.98327
S-70	-0.93969	0	0.34202	0.01938	0.11698	0.99295
S-75	-0.96593	0	0.25882	0.00852	0.06699	0.99772
S-80	-0.98481	0	0.17365	0.00260	0.03015	0.99954
S-85	-0.99619	0	0.08716	0.00033	0.00760	0.99997
S-90	-1.00000	0	0.00000	0.00000	0.00000	1.00000
S-95	-0.99619	0	-0.08716	0.07926	0.99240	0.09409
S-100	-0.98481	0	-0.17365	0.14131	0.96985	0.19857
S-105	-0.96593	0	-0.25882	0.18530	0.93301	0.30847
S-110	-0.93969	0	-0.34202	0.21147	0.88302	0.41899
S-115	-0.90631	0	-0.42262	0.22115	0.82139	0.52574
S-120	-0.86603	0	-0.50000	0.21651	0.75000	0.62500
$\Sigma$ Contraction, 5° angles				2.95759	14.84967	15.48332
$\Sigma$ Contraction, 10° angles				1.50966	7.60287	8.13784
$\Sigma$ Contraction, 15° angles				1.01660	5.18301	5.68472
$\Sigma$ Contraction, 20° angles				0.80579	4.46984	3.99899
$\Sigma$ Contraction, 30° angles				0.49103	2.75000	3.21651
$\Sigma$ Contraction, 40° angles				0.39500	2.36697	2.41492

The mineral plane rotation as well as the contraction of the MCFs in the x, y and z axes are listed as displacements  $u$ ,  $v$  and  $w$  (Table 1). The total angular contraction of the sublamellar MCFs at every 5°, 10°, 15°, 20°, 30° and 40° angles are listed as total displacements  $u_t$ ,  $v_t$  and  $w_t$  for each lamella (Table 1). In this model,  $u_{at}$  was the minimum displacement observed at all angle intervals, while at 5°, 10°, 15° and 30° and 40° intervals,  $w_{at}$ , and at 20° angle intervals,  $v_{at}$  displayed maximum contraction. The AnR ratios of the MCF contraction (as  $w_{at}/v_{at}$  or  $w_{at}/u_{at}$ ) were calculated, listed in Table2 and compared with the literature [10].

**Table 2.** Calculated AnR values derived from total contraction summed at multiples of angles.

	5°	10°	15°	20°	30°	40
$W_{at}/V_{at}$	1.04267	1.07046	1.09679	0.89466	1.16964	1.02026
$W_{at}/U_{at}$	5.23511	5.39051	5.59189	4.96282	6.55054	6.11372
$V_{at}/W_{at}$	0.95908	0.93426	0.91174	1.11774	0.85496	0.98014
$U_{at}/W_{at}$	0.19102	0.18551	0.17883	0.20150	0.15266	0.16357

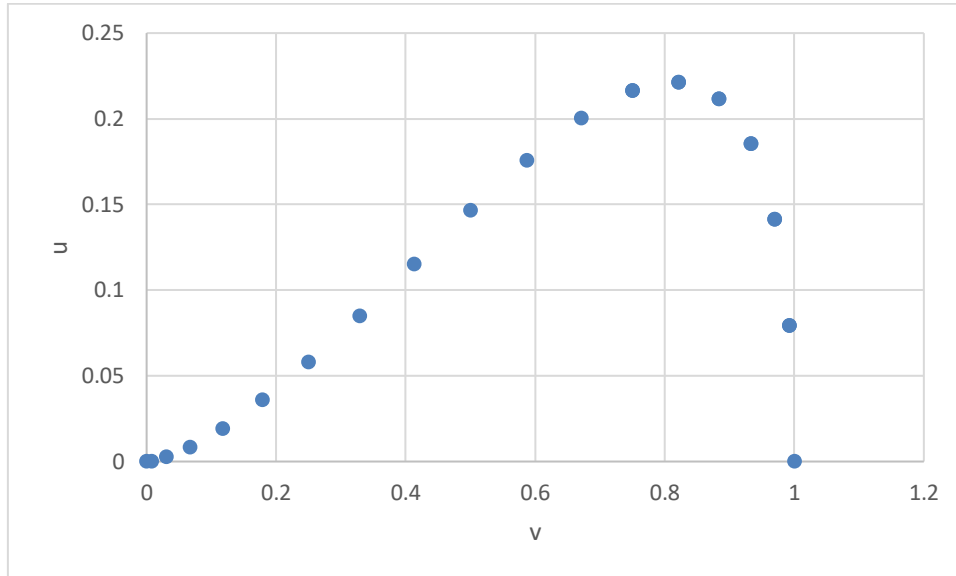


**Figure 5.** The distribution of the  $u$  and  $v$  displacements of the sublamellae at angles ranging from  $0^\circ$  to  $120^\circ$ . The dominant contribution to contraction is from the  $v$  component, while the  $u$  component displays the highest contribution at  $25^\circ$ , i.e. S-05 sublamella.

The distribution of  $u$  and  $v$  displacements (Table 1 and Fig. 5) indicates that the  $v$  component displays higher values than the  $u$  component, implying that the  $v$  displacement is the major contributor to tissue reaction during nanoindentation [10].

## IV. DISCUSSION

In this study, the dehydration-rehydration based contraction in bone lamellae was modelled on the assumption that the collagen contracted towards the mineral plate with dehydration. The model demonstrated the important contribution of the contracted MCF orientation to bone AnR values, which ranged from 0.15266 to 6.55054. Considering the various MCF angular orientations (varying between  $5^\circ$ - $40^\circ$  angles) [9], the results for the MCFs oriented at  $20^\circ$  angles gave an AnR ( $w/v$ ) of 0.89 and an AnR ( $v/w$ ) of 1.12, which correlated to some extent with the experimental AnR data for wet bone of 0.80 and dry bone of 1.13 respectively [10]. The results of this study also indicated a prominent axial contraction, which has not been previously discussed in the literature.

The effect of dehydration-rehydration based contraction on osteonal lamellar bone mechanical properties and anisotropy has been studied in orientations relative to the osteonal axis [6]-[8]. The results indicate differences in lamellar AnR values between the dehydrated and hydrated osteonal bone samples by nanoindentation [10],[29]-[31]. As water associates mainly with collagen in the MCF, dehydration caused contraction involves mainly the compliant element. The capacity of the fibrils to contract or deform [10] is associated here with the compliant element in wet bone, resulting in an AnR<sub>c</sub> ( $w/v$ ) of 0.89. Inversely, in dry bone, the dehydration based AnR ratio is defined as the ratio of resistance to contraction (AnR<sub>r</sub>), or the capacity of the fibrils to resist deformation due to the resistive element in dry bone, resulting in an AnR<sub>r</sub> ( $v/w$ ) of 1.12.

The length scale and MCF orientation are important factors in bone anisotropy as the variation in fibril orientation changes across the osteon from axial (close to the Haversian canal) to angular (towards the cement line) [14], generating prestresses in bone [32]. The aspect of lateral nanoindentation (Fig. 4) may also affect the experimental results [32], which appear to correlate with the  $w/v$  and  $v/w$  AnRs (instead of  $w/u$  and  $u/w$  AnRs) obtained in this study. This implies that results of nanoindentation into Plane 2

may be the summation of tissue response arising from both tangential ( $u_{at}$ ) and radial displacements ( $v_{at}$ ). In fact, the results demonstrate that in all angles the  $v$  displacements, being much larger than the  $u$  displacements, contribute more to the mechanical properties and thus lateral nanoindentation results may be largely governed by the  $v$  displacements (Fig. 5) [8].

In summary, bone properties vary greatly by the length scale, composition, mineral content, sampling site and sample orientation. At the lamellar length scale, the sublamellar patterning may be organized approximately at  $20^\circ$  angles, with a considerable amount of axially arranged contracting elements in the sublamellae, contributing to the osteonal bone mechanical properties than previously discussed.

## **IV. CONCLUSION**

The results of this study indicate presence of not only radially and tangentially but also axially oriented elements sensitive to hydration. According to the results of this theoretical study, anisotropy caused by sublamellar patterning organized at  $20^\circ$  angles affects bone contraction/expansion properties both experimentally and theoretically. The AnR results of the model suggested here imply that the length scale and MCF orientation may be important affectors of the mechanical properties of bone as a hierarchically organized composite.

**ACKNOWLEDGEMENTS:** I would like to thank Dr. Onur Cem Namlı, from the Mechanical Engineering Department, Yeditepe University, Istanbul, Turkey, for his valuable contribution to the confirmation of the results by computation and preliminary reading of this paper.

## **V. REFERENCES**

- [1] R. Robinson and M. L. Watson, "Collagen-crystal relationships in bone as seen in the electron microscope." *Anat. Rec.*, vol. 114, no. 32, pp. 383–410, 1952, doi:10.1002/ar.1091140302.
- [2] A. Ascenzi and E. Bonucci, "The tensile properties of single osteons," *Anat. Rec.*, vol. 158, no. 4, pp. 375-386, 1967, doi: 10.1002/ar.1091580403.
- [3] S. Nomura, A. Hiltner, J. B. Lando, and E. Baer, "Interaction of water with native collagen," *Biopolymers*, vol. 16, no. 2, pp. 231-246, 1977, doi: 10.1002/bip.1977.360160202.
- [4] S. Weiner and H. D. Wagner, "The material bone: Structure mechanical function relations," *Annu. Rev. Mater. Sci.*, vol. 28, pp. 271-298, 1998, doi: 10.1146/annurev.matsci.28.1.271.
- [5] S. C. Cowin, "Mechanosensation and fluid transport in living bone," *J Musculoskelet. Neuronal Interact.*, vol. 2, no. 3, pp. 256-260, 2002.
- [6] V. Ziv, I. Sabanay, T. Arad, W. Traub, and S. Weiner, "Transitional structures in lamellar bone," *Microsc. Res. Techniq.*, vol. 33, no. 2, pp. 203-213, 1996.
- [7] P. Fratzl and R. Weinkamer, "Nature's hierarchical materials," *Prog. Mater. Sci.*, vol. 52, no. 8, pp. 1263-1334, 2007.
- [8] F. S. Utku, E. Klein, H. Saybasili, C. A. Yucesoy, and S. Weiner, "Probing the role of water in lamellar bone by dehydration in the environmental scanning electron microscope," *J. Struct. Biol.*, vol. 162, no. 3, pp. 361-367, 2008, doi: 10.1016/j.jsb.2008.01.004.

- [9] N. Reznikov, R. Shahar, and S. Weiner, "Bone hierarchical structure in three dimensions," *Acta Biomater.*, vol. 10, no. 9, pp. 3815-3826, 2014, doi: 10.1016/j.actbio.2014.05.024.
- [10] A. Faingold, S. R. Cohen, R. Shahar, S. Weiner, L. Rapoport, and H. D. Wagner, "The effect of hydration on mechanical anisotropy. topography and fibril organization of the osteonal lamellae," *J Biomech.*, vol. 47, no. 2, pp. 367-372, 2014, doi: 10.1016/j.jbiomech.2013.11.022.
- [11] M. M. Giraud-Guille, "Twisted plywood architecture of collagen fibrils in human compact-bone osteons," *Calcif. Tissue Int.*, vol. 42, no. 3, pp. 167-180, 1988, doi: 10.1007/BF02556330.
- [12] S. Weiner and W. Traub, "Bone structure: from angstroms to microns," *FASEB J.*, vol. 6, no. 3, pp. 879-895, 1992.
- [13] W. Wagermaier, H. S. Gupta, A. Gourrier, M. Burghammer, P. Roschger, and P. Fratzl, "Spiral twisting of fiber orientation inside bone lamellae," *Biointerphases*, vol. 1, no. 1, pp. 1-5, 2006, doi: 10.1116/1.2178386.
- [14] G. Marotti, "A new theory of bone lamellation," *Calcif. Tissue Int.*, vol. 53, Suppl. 1, pp. S47-S56, 1993, doi: 10.1007/BF01673402.
- [15] J. D. Currey, "The Structure of Bone Tissue," in *Bones: Structure and Mechanics*, 1st. ed. Princeton, NJ, USA: Princeton University Press, 2002, ch. 1, pp. 2- 25.
- [16] H. D. Wagner and S. Weiner, "On the relationship between the microstructure of bone and its mechanical stiffness," *J Biomech.*, vol. 25, no. 11, pp. 1311-1320, 1992, doi: 10.1016/0021-9290(92)90286-a.
- [17] C. J. Newcomb, R. Bitton, Y. S. Velichko, M. L. Snead, and S. I. Stupp, "The role of nanoscale architecture in supramolecular templating of biomimetic hydroxyapatite mineralization," *Small*, vol. 8, no. 14, pp. 2195-2202, 2012, doi: 10.1002/sml.201102150.
- [18] N. Reznikov, R. Shahar, and S. Weiner, "Three-dimensional structure of human lamellar bone: the presence of two different materials and new insights into the hierarchical organization," *Bone*, vol. 59, pp. 93-104, 2014, doi: 10.1016/j.bone.2013.10.023.
- [19] N. Reznikov, J. A. M. Steele, P. Fratzl, and M. M. Stevens, "A materials science vision of extracellular matrix mineralization," *Nat. Rev. Mater.*, vol. 1, Art. no. 16041, 2016, doi: 10.1038/natrevmats.2016.41.
- [20] E. E. Wilson, A. Awonusi, M. D. Morris, D. H. Kohn, M. M. Tecklenburg, and L. W. Beck, "Three structural roles for water in bone observed by solid-state NMR," *Biophys. J.*, vol. 90, no. 10, pp. 3722-3731, 2006, doi: 10.1529/biophysj.105.070243.
- [21] W. J. Landis, M. J. Song, A. Leith, L. McEwen, and B. F. McEwen, "Mineral and organic matrix interaction in normally calcifying tendon visualized in 3 dimensions by high-voltage electron-microscopic tomography and graphic image-reconstruction," *J. Struct. Biol.*, vol. 110, no. 1, pp. 39-54, 1993, doi: 10.1006/jsbi.1993.1003.
- [22] E. D. Eanes, D. R. Lundy, and G. N. Martin, "X-Ray diffraction study of the mineralization of turkey leg tendon," *Calcif. Tissue Res.*, vol. 6, no. 3, pp. 239-248, 1970, doi: 10.1007/BF02196204.
- [23] E. D. Eanes, G. N. Martin, and D. R. Lundy, "The distribution of water in calcified turkey leg tendon," *Calcif. Tissue Res.*, vol. 20, no. 3, pp. 313-316, 1976, doi: 10.1007/BF02546418.

- [24] L. C. Bonar, S. Mook, and H. A. Lees, "Neutron-diffraction studies of collagen in fully mineralized bone," *J. Mol. Biol.*, vol. 181, no. 2, pp. 265-270, 1985, doi: 10.1016/0022-2836(85)90090-7.
- [25] D. Magne, P. Weiss, J. M. Bouler, O. Laboux, and G. Daculsi, "Study of the maturation of the organic (Type I collagen) and mineral (nonstoichiometric apatite) constituents of a calcified tissue (dentin) as a function of location: A Fourier transform infrared microspectroscopic investigation," *J. Bone Miner. Res.*, vol. 6, no. 4, pp. 750-757, 2001, doi: 10.1359/jbmr.2001.16.4.750.
- [26] W. J. Landis, "The strength of a calcified tissue depends in part on the molecular structure and organization of its constituent mineral crystals in their organic matrix," *Bone*, vol. 16, no. 5, pp. 533-544, 1995, doi: 10.1016/8756-3282(95)00076-p.
- [27] M. Fois, A. Lamure, M. J. Fauran, and C. Lacabanne, "Study of human cortical bone and demineralized human cortical bone viscoelasticity," *J. Appl. Polym. Sci.*, vol. 79, no. 14, pp. 2527-2533, 2001, doi: 10.1002/1097-4628(20010401)79:14<2527.
- [28] D. Liu, H. D. Wagner, and S. Weiner, "Bending and fracture of compact circumferential and osteonal lamellar bone of the baboon tibia," *J Mater. Sci. Mater. Med.*, vol. 11, no. 1, pp. 49-60, 2000, doi: 10.1023/a:1008989719560.
- [29] Z. Fan, J. G. Swadener, J. Y. Rho, M. E. Roy, and G. M. Pharr, "Anisotropic properties of human tibial cortical bone as measured by nanoindentation," *J Orthop. Res.*, vol. 20, no. 4, pp. 806-810, 2002, doi: 10.1016/S0736-0266(01)00186-3.
- [30] P. E. Riches, N. M. Everitt, A. R. Heggie, and D. S. McNally, "Microhardness anisotropy of lamellar bone," *J Biomech.*, vol. 30, no. 10, pp. 1059-1061, 1997, doi: 10.1016/s0021-9290(97)00075-4.
- [31] A. Faingold, S. R. Cohen, N. Reznikov, and H. D. Wagner, "Osteonal lamellae elementary units: Lamellar microstructure, curvature and mechanical properties," *Acta Biomater.*, vol. 9, no. 4, pp. 5956-5962, 2013, doi: 10.1016/j.actbio.2012.11.032.
- [32] M-G. Ascenzi, "A first estimation of prestress in so-called circularly fibered osteonic lamellae," *J Biomech.*, vol. 32, no. 9, pp. 935-942, 1999, doi:10.1016/s0021-9290(99)00080-9.